JOURNAL OF SYNCHROTRON RADIATION

ISSN 1600-5775

Observation of scissors modes in solid state systems with a SQUID

Keisuke Hatada,[a,b,c] Kuniko Hayakawa,[c] Fabrizio Palumbo[c] and Augusto Marcelli[c,d]*

[a]Département Matériaux Nanosciences, Institut de Physique de Rennes, UMR UR1-CNRS 6251, Université de Rennes 1, F-35042 Rennes Cedex, France, [b]Physics Division, School of Science and Technology, Università di Camerino, Via Madonna delle Carceri 9, I-62032 Camerino (MC), Italy, [c]INFN Laboratori Nazionali di Frascati, Via E. Fermi 40, CP 13, I-00044 Frascati, Italy, and [d]Rome International Center for Materials Science Superstripes (RICMASS), 00185 Rome, Italy. *Correspondence e-mail: marcelli@lnf.infn.it

Received 7 August 2015
Accepted 21 January 2016

Edited by P. A. Pianetta, SLAC National Accelerator Laboratory, USA

Keywords: rotor model of deformed ions; scissors modes; SQUID; collective magnetic excitations.

The occurrence of scissors modes in crystals that have deformed ions in their unit cells was predicted some time ago. The theoretical value of their energy is rather uncertain, however, ranging between ten and a few tens of eV, with the corresponding widths of 10^{-7} to 10^{-6} eV. Their observation by resonance fluorescence experiments therefore requires a photon spectrometer covering a wide energy range with a very high resolving power. Here, a new experiment is proposed and discussed in which such difficulties are overcome by measuring with a superconducting quantum interference device (SQUID) the variation of the magnetic field associated with the excitation of scissors modes.

1. Introduction

In a series of papers it has been suggested that deformed atoms in crystal unit cells might have collective excitations called scissors modes (Hatada *et al.*, 2005, 2010, 2012). These are states in which two particle systems move with respect to each other conserving their shape. They were first predicted to occur in deformed atomic nuclei (Iudice & Palumbo, 1978) by a semiclassical two-rotor model (TRM) in which protons and neutrons were assumed to form two interacting rotors to be identified with the blades of scissors. Their relative motion (Fig. 1) generates a magnetic dipole moment whose coupling with the electromagnetic field provides their signature.

After their discovery (Bohle *et al.*, 1984) in a rare-earth nucleus, ^{156}Gd, and their systematic experimental and theoretical investigation (Iudice, 2000; Enders *et al.*, 1999) in all deformed atomic nuclei, scissors modes were predicted to occur in several other systems including metal clusters (Lipparini & Stringari, 1989; Portales *et al.*, 2001), quantum dots (Serra *et al.*, 1999), Bose–Einstein (Guéry-Odelin & Stringari, 1999) and Fermi (Minguzzi & Tosi, 2001) condensates and crystals (Hatada *et al.*, 2005, 2010, 2012). In all these systems one of the blades of the scissors must be identified with a moving cloud of particles (electrons in metal clusters and quantum dots, atoms in Bose–Einstein and Fermi condensates, individual atoms in crystal unit cells) and the other one with a structure at rest (the trap in Bose–Einstein and Fermi condensates, the lattice in metal clusters, quantum dots and crystals). The dynamics of such systems can then be described by a one-rotor model (ORM).

More recently the TRM has been used (Hatada *et al.*, 2014) also for single-domain free nanoparticles (Chudnovsky, 1979,

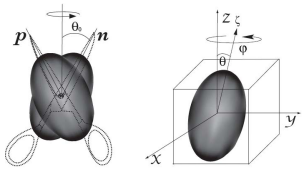

© 2016 International Union of Crystallography

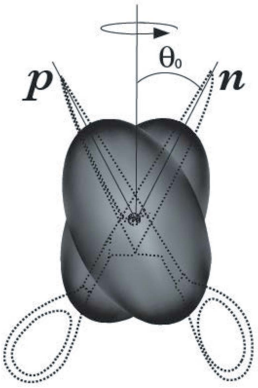

Figure 1
Scissors mode in atomic nuclei: the proton and neutron symmetry axes precess around their bisector.

1992, 1994; Chudnovsky & Gunther, 1988; Grabert & Weiss, 1984; Chudnovsky & Garanin, 1997; Garanin & Chudnovsky, 1997; Friedman, 2003). These objects consist of a magnetic structure, called macrospin, that rotates with respect to a non-magnetic lattice. They have been represented as a couple of rigid rotors, one associated with the non-magnetic lattice and the other one, with a spin attached, with the macrospin. If the nanoparticles are not free, but stuck in rigid matrices, the dynamics are determined by a ORM with spin, representing the macrospin.

Scissors modes have been observed not only in atomic nuclei but also in Bose–Einstein condensates (Maragò *et al.*, 2000). Moreover, nanoparticles stuck in a rigid matrix were studied in detail by a ORM, and the magnetic susceptibility was found to be compatible with a vast body of experimental data and in some cases the agreement was surprisingly good (Hatada *et al.*, 2014). So we can fairly state that the two-rotors or the one-rotor models are relevant to disparate physical systems involving energies and sizes at very different scales.

Scissors modes in crystals have also been studied in the framework of a ORM in which an ion is regarded as a rigid body, which can rotate around the axes of its unit cell under the electrostatic force generated by the ligands. We considered crystals with uniaxial (Hatada *et al.*, 2005) and cubic symmetry (Hatada *et al.*, 2010). In the first case the precessing ion was treated as one ellipsoidal rotor, and in the second case as the body obtained by superimposing three ellipsoids at right angles. In the presence of uniaxial symmetry the photo-absorption cross section is characterized by a linear dichroism (Hatada *et al.*, 2005) (Fig. 2) due to the fact that the ion can rotate around the symmetry axis of the unit cell but not around the other ones.

In the first paper on crystals (Hatada *et al.*, 2005) it was proposed to search for scissors modes with a resonance fluorescence experiment. In such an experiment the dichroism can help to eliminate the background.

Then the case was considered of ions characterized by spin–orbit locking, namely ions in which the spin–orbit force is so strong as to lock the total spin to the density profile in such a way that they rotate together. For such a case a different experiment was proposed, inspired by the experiments on Bose–Einstein condensates (Maragò *et al.*, 2000). In the latter ones one induces oscillations of the condensate giving a sudden twist to the magnetic trap. In the case of ions with spin–orbit locking, one induces oscillations of the ions in the unit cells by an impulsive change of an external magnetic field and observes the photons emitted when the ion moves to the ground state.

The estimate of the energy of scissors modes is affected by a large uncertainty, ranging from ten to a few tens of eV. This makes the experiments difficult, because one has a spectrometer covering a large X-ray energy range with a resolving power up to 10^7. Such a high value is due to the long lifetime of the scissors mode and could explain why, as far as we know, no hint of scissors modes has appeared so far in the experimental measurements of spectra in crystals.

We therefore propose a novel experimental technique suitable for detecting scissors modes excited by an intense source of X-rays. Instead of detecting the photons emitted in the decay, we propose to measure the variation of the magnetic field associated with such excitation. For this purpose we can use a superconducting quantum interference device (SQUID), suitable for measuring extremely small magnetic fields.

The restoring force acting on the ions in our model is mainly due to the interaction of their electric quadrupole moment with the electric quadrupole moments of the ligands. Scissors modes will then be realised more easily in compounds in which there are highly deformed ions, and natural candidates are compounds containing rare-earths (REs). Moreover the *f*-electrons of the REs are compact and for this reason they can be reasonably assimilated to a rigid rotor.

We will consider crystals and gels in which REs are dispersed. The second case is very interesting, because the RE ions are well separated, so as to completely justify our basic approximation that they are not interacting with one another.

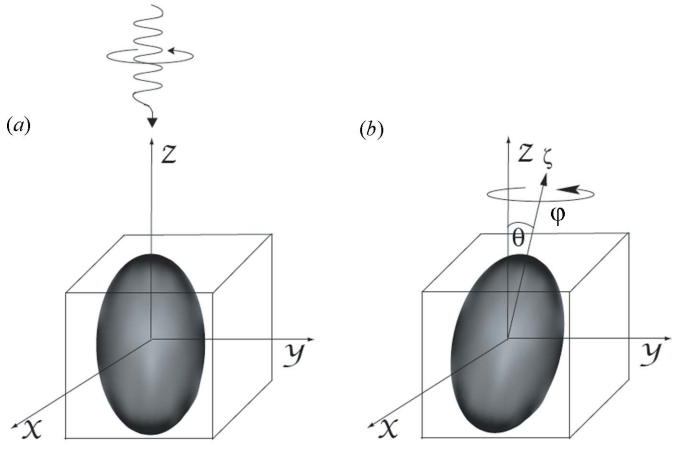

Figure 2
In (*a*) an atom is in its ground state in a unit cell while a photon is incoming with circular polarization and momentum parallel to the axis of the cell. In (*b*) the photon has been absorbed, transferring its angular momentum to the atom, which precesses around the symmetry axis. A photon with momentum orthogonal to the cell axis cannot be absorbed, because the atom cannot absorb its angular momentum since it cannot rotate around any axis orthogonal to the cell axis.

It will turn out, unfortunately, that this type of experiment with gels appears to be below the limit of present possibilities.

We end this introduction by noting the many reasons for the interest in scissors modes. On general grounds for every system scissors modes should affect the dispersive effects in the channels with their quantum numbers, which are $J^\pi = 1^+$. For given systems the scissors modes provide specific pieces of information. In nuclear physics they are related to the superfluidity of deformed nuclei; in Bose–Einstein condensates they provide a signature of superfluidity; in metal clusters they are predicted to be responsible for paramagnetism; in nanoparticles they provide information about the moment of inertia of the macrospin. Knowledge of their properties should be of some consequence also for crystals, because the magnetic anisotropy of these systems is at the origin of many interesting technological applications including magnetic storage devices and sensors, spin-torque nano-oscillators for high-speed spintronics and spin-optics (Smentek & Wybourne, 2007). In particular, one could establish or rule out the existence of spin–orbit locking in RE atoms.

We will start by describing, in §2, the ORM that we will use to describe the dynamics of a deformed atom in a crystal cell or in a gel. Next we will discuss in §3 the estimation of the parameters entering our model. Finally, in §4 we will evaluate the magnetic field generated by photon absorption to be measured by a SQUID, and will present our conclusions in §5.

2. One-rotor model

In the single-ion model of magnetic anisotropy each RE ion is assumed to be independent of the others. In studies of the magnetic properties only the motion of the 4*f* electron system as a whole is considered, disregarding its excitations. In other words this system is treated as a rigid rotor with spin. We introduce the principal frame of inertia of the ion with axes ξ, η, ζ and study its dynamics with respect to a frame of reference fixed with the unit cell with x, y, z-axes parallel to the cell axes. We restrict ourselves to a rotor with axial symmetry and assume the symmetry axis to be parallel to the ζ-axis. In quantum mechanics, rotations around the symmetry axis are forbidden, and therefore the wavefunctions must satisfy the constraint

$$\hat{\boldsymbol{\zeta}} \cdot \mathbf{L}\psi = 0, \tag{1}$$

where $\mathbf{L}$ is the angular momentum of the ion. Its components in the cell frame then become those of a point particle. Assuming the symmetry axis of the ion is along the ζ-axis, the kinetic energy operator is

$$T = \frac{\hbar^2}{2\mathcal{I}}\left(-\frac{\partial^2}{\partial\theta^2} - \cot\theta\frac{\partial}{\partial\theta} + \frac{1}{\sin^2\theta}L_z^2\right) + V, \tag{2}$$

where θ is the angle between the z- and ζ-axes, $L_z = -i\hbar\,\partial/\partial\varphi$ is the z-component of the orbital angular momentum, and $\mathcal{I}$ is the moment of inertia with respect to the ξ- and η-axes. For the potential we assume

$$V = \frac{1}{2}C\sin^2\theta, \tag{3}$$

where C is a restoring force constant.

The scalar product for such a system remains defined by the measure of integration over the Euler angles, which for functions independent of γ is

$$\langle\psi_i|\psi_f\rangle = \int_0^{2\pi} \mathrm{d}\varphi \int_0^{\pi} \mathrm{d}\theta \sin\theta\, \psi_i^*(\theta,\varphi)\,\psi_f(\theta,\varphi) = \delta_{if}. \tag{4}$$

The exact eigenfunctions and eigenvalues are known (Abramowitz & Stegun, 1972), but in cases of physical interest the quadratic approximation is sufficient,

$$\begin{aligned} T &= \frac{\hbar^2}{2\mathcal{I}}\left(-\frac{\partial^2}{\partial\theta^2} - \frac{1}{\theta}\frac{\partial}{\partial\theta} + \frac{1}{\theta^2}L_z^2\right), \qquad 0 \le \theta \le \pi, \\ V &= \begin{cases} (1/2)C\theta^2, & 0 \le \theta \le \pi/2, \\ (1/2)C(\pi-\theta)^2, & \pi/2 < \theta \le \pi. \end{cases} \end{aligned} \tag{5}$$

We recognize that this Hamiltonian, in each of the θ-regions above, is exactly that of a two-dimensional harmonic oscillator, provided we identify θ with the polar radius. As shown by the following estimates, the fall-off of the wavefunction is so fast that we can extend without any appreciable error the integral over θ up to infinity.

In the quadratic approximation, in the region $0 \le \theta \le \pi/2$ the eigenfunctions are

$$\psi_{n,l_z}(\theta,\varphi) = \frac{1}{\sqrt{2\pi}}\exp(il_z\varphi)\,\chi_{n,|l_z|}(\theta), \tag{6}$$

where

$$\chi_{n,|l_z|}(\theta) = \nu_{n,|l_z|}\left(\frac{\theta}{\theta_0}\right)^{|l_z|}\exp\left(-\frac{\theta^2}{2\theta_0^2}\right)L_n^{(|l_z|)}\left(\frac{\theta^2}{\theta_0^2}\right). \tag{7}$$

$L_n^{(|l_z|)}$ are Laguerre polynomials and

$$\nu_{n,|l_z|} = \frac{1}{\theta_0}\left[\frac{2n!}{(n+|l_z|)!}\right]^{1/2}, \qquad \theta_0^2 = \frac{\hbar}{(\mathcal{I}C)^{1/2}}. \tag{8}$$

The eigenvalues are

$$E_{n,l_z} = \hbar\omega(2n + |l_z| + 1) \qquad (n = 0, 1, 2, \ldots), \tag{9}$$

where

$$\omega = (C/\mathcal{I})^{1/2}. \tag{10}$$

The first excited states have $n = 0$, $l_z = \pm 1$, and, as we will see, they are the only states strongly coupled to the ground state by electromagnetic radiation. As shown in Fig. 2, they describe the precession of the atom at an angle $\bar{\theta} \simeq \theta_0$ around the axis of the unit cell.

If the ion is spinless its wavefunction is invariant under the inversion of the orientation of its symmetry axis, that is, not observable. A discussion of the consequences of this symmetry can be found by Palumbo, (2014) but will be ignored here because most RE ions do have a non-vanishing spin.

The dynamics are determined by the magnitude of the zero-point fluctuations θ_0. When $\theta_0 \to 0$ the axis of the rotor can be assumed to lie along the z-axis, the direction of easy magne-

tization, and its zero-point fluctuations can be ignored. For $\theta_0 \simeq 1$, the zero-point fluctuations cannot be neglected, but the rotor is still polarized within an angle of order θ_0. For $\theta_0 \gg 1$, there is no polarization at all.

We quote the values of θ_0 in various systems: in the atomic nuclei (Iudice & Palumbo, 1978) of the REs, $\theta_0^2 \approx 10^{-2}$; in the crystal $LaMnO_3$, $0.1 < \theta_0^2 < 0.5$, depending on how the moment of inertia and restoring force constant are evaluated. Note that in the mentioned compound the deformed ion is Mn.

3. Estimates of the parameters

For numerical evaluations we need estimates of the moment of inertia $\mathcal{I}$ and of the restoring force constant C of the RE ions.

For the moment of inertia we should assume, consistently with our ORM, the expression appropriate to a rigid body,

$$\mathcal{I} = \frac{2}{5} m_e Z \langle r_Z^2 \rangle, \tag{11}$$

where m_e is the electron mass, $\langle r_Z^2 \rangle$ is the mean square radius of the electrons that contribute to the moment of inertia, and Z is their number. We must then establish which are the electrons that effectively take part in the rotation. Indeed one might include or exclude in the evaluation of $\mathcal{I}$ those electrons whose distribution has a spherical shape (Hatada *et al.*, 2012). For a RE this means including or excluding all the electrons of the inner shells and the 4*f*-electrons that have a spherical density. In the presence of locking, however, the 4*f*-electrons that have a spherical distribution have a non-vanishing spin and therefore rotate with the electrons which determine the charge deformation, so that the ambiguity is restricted to the inner shells. If we assume that only the 4*f*-electrons participate in the rotation, we can set $\langle r_Z^2 \rangle = \langle r_{4f}^2 \rangle \approx a_0^2$ ($a_0 \approx 0.5$ Å) and $Z = Z_{4f} \approx 10$ if we consider, for instance, Dy, Ho and Er, thus obtaining

$$\frac{\hbar^2}{\mathcal{I}} \approx 8 \text{ eV}. \tag{12}$$

The main contribution to the restoring force comes from the interaction between the electric quadrupole moment of the RE ion and the electric quadrupole moment of the ligands. So the expression of C depends on the specific structure. One example of its calculation is given by Hatada *et al.* (2005), but here we do not want to restrict ourselves to particular cases. Therefore we will avoid the evaluation of C and parametrize the energy of the scissors modes according to

$$E_S = \hbar \left(\frac{C}{\mathcal{I}} \right)^{1/2} = \frac{\hbar^2}{\mathcal{I}} \frac{1}{\theta_0^2} > 8\theta_0^{-2} \text{ eV}. \tag{13}$$

We will assume that θ_0^2 must be smaller than 1 if the RE ion must be polarized, and in specific cases we indeed found $\theta_0^2 \approx 0.5$.

It is also interesting to estimate the resolution power for our experiment. The expression of the width of the scissors mode was determined by Hatada *et al.* (2010, 2012),

$$\Gamma \approx \frac{3}{4} \alpha \left(\frac{\hbar^2}{\mathcal{I}} \right)^3 \frac{1}{(m_e c^2)^2} \theta_0^{-8} > 1.6 \times 10^{-10} \text{ eV}. \tag{14}$$

Notice the strong dependence on θ_0. With our parametrization of the energy we obtain

$$\frac{E_S}{\Gamma} = \frac{4}{3\alpha} \left(\frac{m_e c^2 \mathcal{I}}{\hbar^2} \right)^2 \theta_0^6 = 6 \times 10^8 \theta_0^6 < 7 \times 10^7. \tag{15}$$

We must note that the above expression is not entirely consistent, because, while the expression of the scissors mode energy has a general validity, the width was evaluated for a specific structure of the crystal cell. Nevertheless, we think it should be sufficient to give an order of magnitude of the resolving power.

4. Estimate of the magnetic field generated by photon absorption

We assume that all the crystal unit cells have their easy axis parallel to the z-axis of the laboratory frame. This situation is realised in single crystals and can be easily achieved by applying a convenient magnetic field. Otherwise an average over the cell axes should be performed, as given by Hatada *et al.* (2014). We also assume that the photons are circularly polarized (left or right is not relevant). The change of the magnetic moment of the target is given by the probability to excite a scissors mode multiplied by the scissors mode magnetic moment minus the ground-state magnetic moment. It can be seen that the spin contribution is θ_0^4 times smaller than the orbital one and therefore will be neglected. The orbital magnetic moment in the ground state vanishes and then

$$\Delta\mu_z = w t_{\text{flux}} N_a \left\langle \psi_{0l_z} \left| \frac{1}{\hbar} L_z \right| \psi_{0l_z} \right\rangle \mu_B, \tag{16}$$

where t_{flux} is the duration of the photon flux, N_a is the effective number of atoms in the sample, μ_B is the Bohr magneton and w is the photon absorption probability per unit time per unit frequency, that is given by

$$w = 4\pi^2 \alpha N(\omega) \frac{\hbar^2 c}{m_e^2 \omega} \left| [M_\varepsilon(\omega)]_{fi} \right|^2. \tag{17}$$

In the above equation, m_e is the electron mass, α the fine-structure constant, c the velocity of light, $N(\omega)$ the number of photons of energy ω per unit volume and $M(\omega)$ the magnetic dipole moment matrix element,

$$(M_\varepsilon)_{fi} = -\frac{\omega}{2c} \left\langle \psi_f \left| \frac{1}{\hbar} L_\varepsilon \right| \psi_i \right\rangle, \tag{18}$$

where

$$L_\varepsilon = -\frac{1}{\sqrt{2}} \exp(\pm i\varphi) \left(\frac{\partial}{\partial\theta} + i\varepsilon \cot\theta \frac{\partial}{\partial\varphi} \right) \tag{19}$$

and $\varepsilon = \pm 1$ is the photon polarization.

Using the expression of the wavefunctions, for the quantum numbers $f = (0, m)$, $i = (00)$,

$$\left(M_{\varepsilon}\right)_{0l_z,00} = -\frac{i\omega}{2\sqrt{2}c\theta_0}\,\delta_{\varepsilon,l_z}, \tag{20}$$

$$\left\langle \psi_{ol_z}\left|\frac{1}{\hbar}L_z\right|\psi_{0l_z}\right\rangle = l_z, \qquad l_z = \pm 1, \tag{21}$$

so that

$$w = \frac{\pi^2}{2}\,\alpha\,\frac{1}{\theta_0^2}\,\lambda_e^2\,\frac{\omega}{\Delta\omega}\,\frac{N_{\rm phot}}{S_{\rm source}}, \tag{22}$$

where λ_e is the Compton wavelength of the electron, ω the photon frequency, $\Delta\omega$ the frequency spread, $N_{\rm phot}$ the number of incoming photons per unit time and $S_{\rm source}$ the cross section of the photon beam.

The effective number of atoms is given by

$$N_a = \rho\lambda_{\rm phot}S_{\rm samp}, \tag{23}$$

where ρ is the number of atoms per unit volume, $S_{\rm samp}$ is the sample surface and $\lambda_{\rm phot}$ is the photon r.m.s. path. The above formula holds provided $\lambda_{\rm phot}$ is smaller than the sample thickness.

We assume the bandwidth to be proportional to the photon frequency according to

$$\Delta\omega = f\omega_{\rm phot} = f\omega_{\rm sciss}, \tag{24}$$

so that finally

$$|\Delta\mu_z| = \frac{\pi^2}{2}\,\alpha\,\frac{1}{\theta_0^2}\,\frac{1}{f}\,N_{\rm phot}\,t_{\rm flux}\,\frac{S_{\rm samp}}{S_{\rm source}}\,\lambda_e^2\,\lambda_{\rm phot}\,\rho\mu_B. \tag{25}$$

A reasonable assumption is that

$$S_{\rm source} \approx S_{\rm samp}, \qquad f = 10^{-3}, \tag{26}$$

so that

$$|\Delta\mu_z| = \frac{\pi^2}{2}\,\alpha\,\frac{1}{\theta_0^2}\,N_{\rm phot}\,t\,\lambda_e^2\,\lambda_{\rm phot}\,\rho\,10^3\mu_B. \tag{27}$$

The strength of the magnetic field along the z-axis generated by this variation of the magnetic moment at a distance r is

$$B_z = \frac{\Delta\mu_z}{r^3}\,\mu_0, \tag{28}$$

where μ_0 is the vacuum magnetic permeability.

Next we assume

$$N_{\rm phot} \approx 10^{11}\ {\rm s}^{-1}, \tag{29}$$

$$\theta_0^2 < 0.5. \tag{30}$$

To proceed further with numerical estimates we must distinguish the case of a dense RE compound sample as a crystal from the case of gels containing highly diluted RE atoms.

All the following numerical estimates will be carried out in SI units. Then

$$\mu_0 = 1.25 \times 10^{-6}\ {\rm H\,m^{-1}}, \qquad \mu_B = 9.3 \times 10^{-24}\ {\rm J\,T^{-1}} \tag{31}$$

and

$$\lambda_e = 4 \times 10^{-13}\ {\rm m}. \tag{32}$$

4.1. Dense matter

We assume one RE atom per unit cell and a cell volume of $(3.5A)^3 = 4.3 \times 10^{-29}$ m^3, so that $\rho_{\rm RE} = 2.3 \times 10^{28}$ m^{-3}.

We then have

$$|\Delta\mu_z| = 7 \times 10^{12}\,t_{\rm flux}\,\lambda_e^2\,\lambda_{\rm phot}\,\rho\mu_B \tag{33}$$

and

$$B = 7 \times 10^{12}\,t_{\rm flux}\,\lambda_e^2\,\lambda_{\rm phot}\,\rho r^{-3}\mu_0\mu_B. \tag{34}$$

Setting

$$\lambda_{\rm phot} \simeq 10^{-4}\ {\rm m}, \qquad r \simeq 10^{-2}\ {\rm m}, \tag{35}$$

we obtain

$$B \simeq 4 \times 10^{-11}\,t_{\rm flux}\ {\rm T}, \tag{36}$$

where $t_{\rm flux}$ is in seconds. Assuming an acquisition of 1 h, we should measure a magnetic moment of the order of 10^{-7} T, which is lower than the Earth's magnetic field on the surface, whose magnitude ranges from 20 to 100 µT. However, we can increase the signal by reducing the distance r of the detector and increasing the acquisition time and the flux intensity.

Examples of suitable compounds for the proposed experiments are $R_2Fe_{14}B$ and $R_2Fe_{17}N_3$ in which the RE ions can be Dy, Ho and Er. We remind that the spin contribution to the variation of the magnetic moment is θ_0^4 times smaller than the orbital contribution. Since all the quoted REs have $Z_{4f} \simeq 10$ and $gJ \simeq 10$, if θ_0 is not sufficiently small the spin contribution cannot be neglected.

Finally, we remark that the ions Gd^{3+} and La^{3+}, being spherical, do not have an orbital response. They can then be used to exclude, by comparison, spurious effects.

4.2. Soft matter

The difference with respect to a crystal is due to the difference of RE density and photon r.m.s. path,

$$B_{\rm gel} = B_{\rm crystal}\,\frac{(\rho_{\rm RE})_{\rm gel}}{(\rho_{\rm RE})_{\rm crystal}}\,\frac{(\lambda_{\rm phot})_{\rm gel}}{(\lambda_{\rm phot})_{\rm crystal}}. \tag{37}$$

If x is the percentage in weight of RE atoms in a gel made of $N_{\rm gel}$ atoms of mass $m_{\rm gel}$,

$$(\rho_{\rm RE})_{\rm gel}\,m_{\rm RE} = x\rho_{\rm gel}\,m_{\rm gel}. \tag{38}$$

Assuming $m_{\rm gel}/m_{\rm RE} \simeq 0.1$, $\rho_{\rm gel} \simeq 0.5 \times 10^{21}$ m^{-3},

$$(\rho_{\rm RE})_{\rm gel} \approx x\,0.5 \times 10^{-9}\,(\rho_{\rm RE})_{\rm crystal}. \tag{39}$$

With a percentage in weight of $x = 0.05$ we will have a magnetic moment $B \approx 10^{-21}\,t_{\rm flux}$ T. Considering that 10^{-15} T is the minimum value of the magnetic field actually detectable by existing SQUID devices, we should imagine an acquisition of tens or even hundreds of hours or reduce significantly the distance and increase the flux intensity to be able to detect a signal from such a diluted RE system.

5. Conclusion

The previous experiments designed to observe scissors modes in dense matter are affected by two orders of difficulty. The first one is the detection of photons in a wide energy spectrum, due to the uncertainty in the theoretical value of the energy of these excitations, that ranges between ten and a few tens of eV. The second one is the need of a resolving power of the order of 10^7, much larger than that routinely used, that is of the order of 10^2 to 10^4. These difficulties might also explain why, if scissors modes exist, they have not been noticed until now.

We propose here an original approach based on a new experimental layout in which, instead of detecting the decay photons, one has to measure with a sensitive SQUID detector the magnetic field associated with the excitation of scissors modes induced by photon absorption. For such an experiment we only need a sufficient flux of photons and a spectrum of the source sufficiently wide to cover the theoretical range of the scissors modes energy.

The experimental method we propose here should help to eliminate spurious signals and will offer several advantages over routinely used techniques:

(i) There should be no magnetic response with a source of linearly polarized photons.

(ii) The intensity of the variation of the magnetic field should decrease as the inverse of the cubic distance between the SQUID sensor and the sample.

(iii) There should be no magnetic response from spherical RE ions.

(iv) Because our calculations are performed assuming that the unit cells axes are aligned, the induced variation of magnetic field should be proportional to the square of the cosine of the angle between the direction of the photons and the easy axes of the cells.

In single crystals, ion axes are naturally aligned while in other systems a suitable alignment can be achieved by applying an external magnetic field. As far as RE dispersed in gels matrices are concerned, it appears possible to synthesize samples with a significant alignment. However, if the direction of the unit cells axes are disordered, we must perform an average, as performed by Hatada *et al.* (2014) for nanoparticles. Obviously such an average does not change the order of magnitude of the results.

In this work we separately considered both dense compounds and light systems such as RE ions dispersed in a gel matrix. In the first case with the available photon fluxes in a synchrotron radiation facility in the ultraviolet energy range, we estimated the variation of the magnetic field to be of the order of 10^{-7} T. This value has to be compared with the typical precision of measurement of the terrestrial magnetic field that is of the order of nanoTeslas.

In the second case, with a small amount of RE ions dispersed in a gel matrix, our estimate yields a magnetic field whose magnitude is well beyond the sensitivity of these superconducting devices. Our approach in this case, although unfeasible at present, is much more interesting from a theoretical point of view. Indeed, for such dilute systems our basic assumption that the RE ions are independent of one another is completely justified and therefore the theoretical interpretation of the results is much cleaner. Experiments on gels, however, could soon become feasible by improving the experimental layout, *e.g.* with a smaller device–sample distance, improving the SQUID with a dedicated design or, in the future, using a free-electron laser source in order to have a photon flux in the ultraviolet energy range three to four orders of magnitude higher then that available with a storage ring.

This original approach can be easily tested and become a powerful technique that we think might be used for the investigation and search of similar behaviours, which may occur in many other systems, in particular in actinides samples in which paramagnetic and deformed atoms can be present in different concentrations.

References

Abramowitz, M. & Stegun, I. A. (1972). *Handbook of Mathematical Functions*, p. 753. New York: Dover.

Bohle, D., Richter, A., Steffen, W., Dieperink, A. E. L., Lo Iudice, N., Palumbo, F. & Scholten, O. (1984). *Phys. Lett. B*, **137**, 27–31.

Chudnovskii, E. M. (1979). *J. Exp. Theor. Phys.* **50**, 1035.

Chudnovsky, E. M. (1992). *Phys. Rev. A*, **46**, 8011–8014.

Chudnovsky, E. M. (1994). *Phys. Rev. Lett.* **72**, 3433–3436.

Chudnovsky, E. M. & Garanin, D. A. (1997). *Phys. Rev. Lett.* **79**, 4469–4472.

Chudnovsky, E. M. & Gunther, L. (1988). *Phys. Rev. Lett.* **60**, 661–664.

Enders, J., Kaiser, H., von Neumann-Cosel, P., Rangacharyulu, C. & Richter, A. (1999). *Phys. Rev. C.* **59**, R1851–R1854.

Friedman, J. R. (2003). *Resonant Magnetization Tunneling in Molecular Magnets*, in *Exploring the Quantum/Classical Frontier: Recent Advances in Macroscopic and Mesoscopic Quantum Phenomena*, edited by J. R. Friedman and S. Han. Huntington: Nova Science.

Garanin, D. A. & Chudnovsky, E. M. (1997). *Phys. Rev. B*, **56**, 11102.

Grabert, H. & Weiss, U. (1984). *Phys. Rev. Lett.* **53**, 1787–1790.

Guéry-Odelin, D. & Stringari, S. (1999). *Phys. Rev. Lett.* **83**, 4452–4455.

Hatada, K., Hayakawa, K., Marcelli, A. & Palumbo, F. (2014). *Phys. Chem. Chem. Phys.* **16**, 24055–24062.

Hatada, K., Hayakawa, K. & Palumbo, F. (2005). *Phys. Rev. B*, **71**, 092402.

Hatada, K., Hayakawa, K. & Palumbo, F. (2010). *Eur. Phys. J. B*, **77**, 41–45.

Hatada, K., Hayakawa, K. & Palumbo, F. (2012). *Eur. Phys. J. B*, **85**, 183.

Iudice, N. L. (2000). *Riv. Nuov. Cim.* **23**, 1.

Iudice, N. L. & Palumbo, F. (1978). *Phys. Rev. Lett.* **41**, 1532–1534.

Lipparini, E. & Stringari, S. (1989). *Phys. Rev. Lett.* **63**, 570–572.

Maragò, O. M., Hopkins, S. A., Arlt, J., Hodby, E., Hechenblaikner, G. & Foot, C. J. (2000). *Phys. Rev. Lett.* **84**, 2056–2059.

Minguzzi, A. & Tosi, M. P. (2001). *Phys. Rev. A*, **63**, 023609.

Palumbo, F. (2014). arXiv:1409.7298.

Portales, H., Duval, E., Saviot, L., Fujii, M., Sumitomo, M. & Hayashi, S. (2001). *Phys. Rev. B*, **63**, 233402.

Serra, Ll., Puente, A. & Lipparini, E. (1999). *Phys. Rev. B*, **60**, R13966–R13969.

Smentek, L. & Wybourne, B. G. (2007). *Optical Spectroscopy of Lanthanides: Magnetic and Hyperfine Interactions.* Boca Raton: CRC Press.